The Electric Quadrupole Contribution to the Circular Birefringence of Nonmagnetic Anisotropic Chiral Media: A Circular Waveguide Experiment

Isak Petrus Theron and Johannes Hendrik Cloete

Abstract— **Constitutive relations which include electric quadrupole terms, in addition to electric and magnetic dipole terms, are used to describe the "optical activity," in particular the circular birefringence, of an anisotropic chiral medium which is nonmagnetic. The resulting permittivity and chirality tensors are then used to predict the rotation of the polarization plane of a linearly polarized wave propagating in a circular waveguide filled with the medium. The numerical predictions were tested by measurements between 2.4 and 4 GHz on a 2 m long artificial crystal in a circular waveguide and it was found that the rotation of the polarization was within 13% of the predicted value—good agreement after considering the possible sources of error. It is thus established that the effect of electric quadrupoles must be included when modeling the optical activity of anisotropic chiral media in the long wavelength regime. The anisotropic chiral media which are dealt with here can be classified according to the crystallographic point groups to which they belong, and they may therefore also be considered to be artificial crystals.**

I. Introduction

THE 1979 paper by Jaggard *et al.* [1] is often cited as a key paper in the microwave engineering literature on artificial chiral media and their possible applications [2], [3]. In their paper, Jaggard *et al.* give a phenomenological explanation of the optical activity of an artificial isotropic chiral medium, composed of randomly oriented conducting helices embedded randomly in an isotropic dielectric host. The resulting constitutive relations $\vec{D} = \epsilon\vec{E} - j\xi\vec{B}$ and $\vec{H} = \mu^{-1}\vec{B} - j\xi\vec{E}$, are often called the Post relations [2] because they appear in Post's 1962 book [4, p. 172]. Only the induced magnetic and electric dipole moments were considered in the physical model of Jaggard *et al.* although molecular physicists and chemists already knew, a decade earlier, that electric quadrupoles may also contribute to optical activity [5], [6]. However, as also shown by Nakano and Kimura [5] and Buckingham and Dunn [6], the individual contributions of the induced electric quadrupole moments cancel due to macroscopic averaging, in the case of a "random" or isotropic medium as considered by Jaggard *et al.* Thus their model was appropriate, although it is not clear that they had considered the effect of the electric quadrupoles and found it to be negligible.

Interest in synthetic anisotropic chiral materials is growing and to deal with them theoretically the constitutive relations for the isotropic case are usually generalized by allowing the scalar parameters to become second rank tensors, e.g., [7]–[11]. However, the physical validity of the resulting description can not be taken for granted because now the effects of the electric quadrupoles are cumulative [5], [6] and must be taken into account.

In 1992 Graham, Pierrus and Raab [12] showed that origin independence requires that electric quadrupole moments must also be included when magnetic dipole moments are considered in multipole descriptions of nonmagnetic matter. A theory is origin independent if its predictions are independent on the location of the origin to which the multipole moments are referred. This form of translational invariance is considered to be an essential feature in theories of modern physics.

Accordingly, Raab and Cloete [13] used constitutive relations, expressed in the electric quadrupole—magnetic dipole approximation, to study the optical activity of nonmagnetic chiral crystals and gases. Subsequently Graham and Raab [14] and Theron [15], [16] showed that the constitutive relations derived from the multipole tensors can be written in the form

$$\vec{D} = \bar{\epsilon}\cdot\vec{E} + j\bar{\xi}\cdot\vec{B} \tag{1}$$

$$\vec{H} = j\bar{\xi}^{T}\cdot\vec{E} + \mu_o^{-1}\vec{B} \tag{2}$$

where

$$\epsilon_{\alpha\beta} = \epsilon_o\delta_{\alpha\beta} + \alpha_{\alpha\beta}$$

$$\xi_{\alpha\beta} = G'_{\alpha\beta} - \tfrac{1}{2}\,\omega\epsilon_{\beta\gamma\delta}\mathrm{a}_{\gamma\delta\alpha}$$

with $\alpha_{\alpha\beta}, G'_{\alpha\beta}$ and $\mathrm{a}_{\alpha\beta\gamma}$ the polarizability tensors characterising the medium. They result from, respectively, the electric dipole, the magnetic dipole and the electric quadrupole moments. Here the Einstein notation [17, Appendix B] is used. Greek subscripts denote any of the Cartesian coordinates with a repeated subscript implying a summation over the three coordinates. The Kronecker delta, $\delta_{\alpha\beta}$, equals 1 when $\alpha = \beta$ and zero otherwise, and $\epsilon_{\beta\gamma\delta}$ is the Levi–Civita or alternating tensor [17, Appendix B]. The time convention $\exp(+j\omega t)$ is implicit.

This theory, being generally applicable to both anisotropic and isotropic matter, was used here to determine the influence of the electric quadrupole term in modeling anisotropic chiral media.

It is emphasized that although the "chirality parameter" $\bar{\xi}$ in (1) and (2) appears to arise from a simple generalization of the Post constitutive relations for isotropic chiral matter, it

Manuscript received December 4, 1995; revised April 19, 1996.

The authors are with the Department of Electrical and Electronic Engineering, University of Stellenbosch, Stellenbosch 7600, South Africa.

Publisher Item Identifier S 0018-9480(96)05650-5.

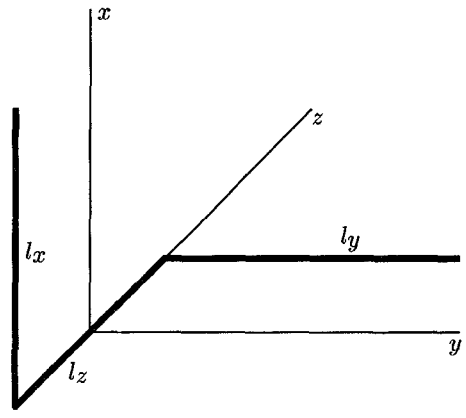

Fig. 1. An elementary chiral structure or enantiomorph.

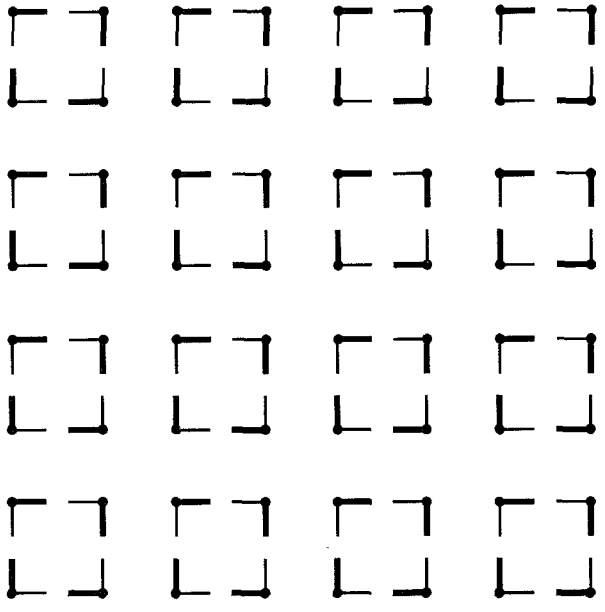

Fig. 2. A uniaxial lattice in the 422 point group. The crystal is constructed by repeating this layer in the z-direction.

explicitly includes the contribution of the electric quadrupoles, in addition to that of the magnetic dipole moments.

II. An Artificial Crystal and Its Constitutive Relations

Anisotropic media which exhibit chiral activity at microwave frequencies apparently do not occur naturally. However, an artificial crystal can be made by arranging small chiral structures, or enantiomorphs, on a regular lattice subject to certain symmetry requirements [15], [16]. A practical crystalline medium was made by embedding the simple chiral structure in Fig. 1 in a point group 422 lattice [18] as shown in Fig. 2.

The medium is fairly dilute to ensure simple coupling between neighboring structures so that the multipole densities can be calculated from the multipole moments of a single structure. It is also required that the frequencies be kept low enough for the medium to resemble a continuum rather than a diffraction grating. The treatment is thus restricted to the low frequency regime [13]. However, the dimensions and spacing of the chiral objects are chosen to make experimentation practical at microwave frequencies, thus the frequencies are not "low" in an absolute sense.

The 2 to 4 GHz band was chosen for the experiments and it was required that the total length of the individual chiral hooks be about 9 mm to ensure that they would be excited far below the half-wave resonance frequency. Thus a medium was constructed using structures with $l_x = l_y = 3.12$ mm and $l_z = 3.14$ mm made from phosphor-bronze wire with diameter 0.3 mm. The structures were spaced 9.3 mm in the z-direction, and 6.5 and 8 mm, respectively, in the tangential plane depicted in Fig. 2. The multipole tensors for this medium were computed using an electroquasistatic moment method formulation [15], [19], resulting in

$$\alpha_{xx} = \alpha_{yy} = 4.48 \times 10^{-13}\ \text{C/Vm}$$
$$\alpha_{zz} = 8.29 \times 10^{-13}\ \text{C/Vm}$$
$$G'_{xx} = G'_{yy} = -\omega\, 1.16 \times 10^{-16}\ \text{A/V}$$
$$G'_{zz} = 0$$
$$\mathrm{a}_{xzy} = \mathrm{a}_{xyz} = -\mathrm{a}_{yxz} = -\mathrm{a}_{yzx} = -2.34 \times 10^{-16}\ \text{C/V}$$

and

$$\epsilon_{xx} = 1.01 \times 10^{-11}\ \text{C/Vm} = 1.14\epsilon_o$$
$$\epsilon_{zz} = 1.06 \times 10^{-11}\ \text{C/Vm} = 1.20\epsilon_o$$
$$\xi_{xx} = -\omega\, 2.54 \times 10^{-16}\ \text{A/V}$$
$$\xi_{zz} = \omega\, 2.55 \times 10^{-16}\ \text{A/V}$$

where the structures have been embedded in a dielectric foam having $\epsilon_r = 1.09$ for manufacturing purposes. It is evidently predicted that the electric quadrupole term $\mathrm{a}_{\alpha\beta\gamma}$, makes a significant contribution. Indeed, since $G'_{xx} \approx \frac{1}{2}\,\omega \mathrm{a}_{xyz}$, neglect of the electric quadrupole reduces the predicted value for the tangential chirality parameter, ξ_{xx}, by approximately half.

The analysis of a linearly polarized plane wave propagating through an unbounded medium characterized by these parameters reveals that the polarization plane will rotate by about 6.5 degrees per meter [15], [16]. It would be highly impractical to measure this using a free space system, thus waveguide measurements were preferred.

The remaining burden of this paper is a description of the circular waveguide experiment, and the supporting theory, which tests the above prediction.

III. Waveguide Propagation

Waveguides filled with isotropic chiral media—so-called chiro-waveguides—have received considerable attention [20]–[23]. An anisotropic medium with dyadic permittivity and permeability, but a scalar chirality parameter, is studied in [7], while [24] considers a medium where the chirality dyadic has zero diagonal terms as would be produced by a crystalline distribution of the so-called Ω-medium [25]. A general solution is also given in [26] using series expansions related to the modes in a nonchiral waveguide. As will be shown later, the rotation of the polarization plane is due to the difference in the propagation constants of the two dominant modes. Since this difference is much smaller than

the constants themselves, a solution which does not require a series expansion is presented here.

The propagation constant inside a rectangular waveguide filled with an isotropic chiral medium is solved numerically in [27], [28] and analytically, using a series of sinusoidal functions, in [29]. Thus the solution for a rectangular waveguide requires either an approximate series or a numeric solution, while that for the circular waveguide can be found analytically. A circular waveguide was therefore chosen for the experiment. Although the medium parameters discussed above are defined for Cartesian coordinates, they remain the same for cylindrical coordinates since the tangential components are independent of direction [15].

The fields in the waveguide can now be found by solving Maxwell's equations subject to the boundary conditions and the constitutive relations in (1) and (2). Appendix A gives the fields satisfying the boundary condition $E_z = 0$ at $r = a$ for an assumed z-dependence of the form $e^{-\jmath\beta z}$ where $\beta = \beta' + j\beta''$ is an unknown constant of propagation. The fields in the waveguide must also satisfy the boundary condition $E_\phi = 0$ at $r = a$ and the value of β is determined to satisfy this condition. Setting $r = a$ in (14) and writing $J_{n-1}[x]$ in terms of $J_n[x]$ and $J_{n+1}[x]$ results in

$$h_b J_{n+1}[k_g a] + h_c J_n[k_g a] J_n[k_f a] - h_a J_n[k_g a] J_{n+1}[k_f a] = 0 \tag{3}$$

where

$$h_a = k_f \left\{ f' k_\beta^2 - \frac{\mu_o}{\epsilon_{xx}} (k_\beta^2 (\xi_{xx} + \xi_{zz}) + 2\beta^2 \xi_{xx})^2 \right\}$$

$$h_b = k_g \left\{ g' k_\beta^2 - \frac{\mu_o}{\epsilon_{xx}} (k_\beta^2 (\xi_{xx} + \xi_{zz}) + 2\beta^2 \xi_{xx})^2 \right\}$$

$$h_c = \frac{n}{a} (f' - g') (k_\beta^2 - 2\omega\mu_o \beta \xi_{xx})$$

with the constants as defined in Appendix A. The solution for β will, in general, be complex. (It is possible to have complex β even in lossless media—the modes are then referred to as complex modes [30]–[32].) For each value of n, β can have multiple solutions each of which represents a hybrid mode that will be able to propagate in the waveguide. Here the modes will be denoted T_{nm}, where m indicates the mth solution of β for a given n. A bar above the n indicates that n is negative; for example, $T_{\bar{1}1}$ is the mode with the first solution of β when $n = -1$.

For nonchiral waveguide modes where the propagation constant is either purely real or purely imaginary, the cut-off frequency can be defined as the frequency for which $\beta = 0$. Setting $\beta = 0$ in (3) and solving for frequency, yields a real valued result. Thus at this frequency, f_c, the modes are not complex and f_c is defined as the cut-off frequency. For chiral guide it was found that f_c is the same for the T_{nm} and $T_{\bar{n}m}$ modes. It was also discovered that at f_c one of the two modes, either T_{nm} or $T_{\bar{n}}m$, in addition to $\beta = 0$ has a positive real solution of β. This is the propagation constant for the particular mode—thus it has a nonzero propagation constant at cut-off and will be able to propagate at frequencies slightly below cut-off. For the parameters considered here this applies to frequencies within $10^{-4}\%$ of f_c.

TABLE I
CUT-OFF FREQUENCIES IN GHz FOR A CHIRAL WAVEGUIDE WITH DIAMETER 79 mm, AND $\epsilon_{xx} = 1.01 \times 10^{-11}$ C/Vm, $\epsilon_{zz} = 1.06 \times 10^{-11}$ C/Vm, $\xi_{xx} = -\omega 2.54 \times 10^{-16}$ A/V AND $\xi_{zz} = \omega 2.55 \times 10^{-16}$ A/V. THE CUT-OFF FREQUENCIES FOR THE $T_{\bar{n}m}$ MODES ARE THE SAME AS THOSE FOR THE T_{nm} MODES. FOR COMPARISON, THE CUT-OFF FREQUENCIES FOR A WAVEGUIDE FILLED WITH A HOMOGENEOUS, NONCHIRAL MEDIUM WITH $\epsilon = \epsilon_{xx}$ ARE ALSO GIVEN

T_{11}	2.08	T_{12}	4.23	T_{13}	6.03
TE_{11}	2.08	TM_{11}	4.33	TE_{12}	6.03
T_{01}	2.65	T_{02}	4.33	T_{03}	6.09
TM_{01}	2.72	TE_{01}	4.33	TM_{02}	6.24
T_{21}	3.45	T_{22}	5.67	T_{23}	7.58
TE_{21}	3.45	TM_{21}	5.81	TE_{22}	7.59
T_{31}	4.75	T_{32}	7.04		
TE_{31}	4.75	TM_{31}	7.22		

Using the parameters from Section II and a waveguide radius of $a = 39.5$ mm in (3) yields the cut-off frequencies for the first few modes as shown in Table I. The cut-off frequencies for a waveguide filled with a homogeneous, nonchiral dielectric with $\epsilon = \epsilon_{xx}$ are given for comparison.

There is a close correspondence between the cut-off frequencies of the chiral waveguide and the nonchiral waveguide, as can be expected for the small values of the chirality parameters used here. (Caveat: consideration of only the first two decimals will lead to the incorrect conclusion that the correspondence is exact.) The field distributions will be similar for modes with closely related cut-off frequencies. The fact that each nonchiral mode is paired with a chiral mode, indicates that the solution of (3) yields all the modes in the chiral waveguide. In accordance with propagation in isotropic waveguide it thus follows that the dominant modes are T_{11} and $T_{\bar{1}1}$.

IV. ROTATION OF THE POLARIZATION PLANE

From the expressions for the fields inside the waveguide (13) to (15) it follows that the $T_{\bar{1}1}$ and T_{11} modes have the same field distribution on the interface, one rotating clockwise and the other anti-clockwise on this plane. As the field distribution of these two modes closely resemble that of the TE_{11} mode, it may be assumed that these two modes will be excited with essentially equal amplitudes by a TE_{11} mode incident on an air–chiral interface inside the waveguide and that only extremely weak higher order modes will be excited. The rotation is therefore caused by the difference in the propagation constants of these two modes only. As can be seen from the ϕ- and z-dependence, the ϕ-distribution rotates by $\beta' z$ radians in the clockwise direction for the T_{11} mode, and in the anti-clockwise direction for the $T_{\bar{1}1}$ mode. Thus the rotation of the polarization plane for the sum of these two modes is

$$\phi_{\mathrm{rot}} = \tfrac{1}{2} (\beta_1' - \beta_{\bar{1}}') \tag{4}$$

radians per meter. The positive ϕ direction is defined as for the conventional polar angle.

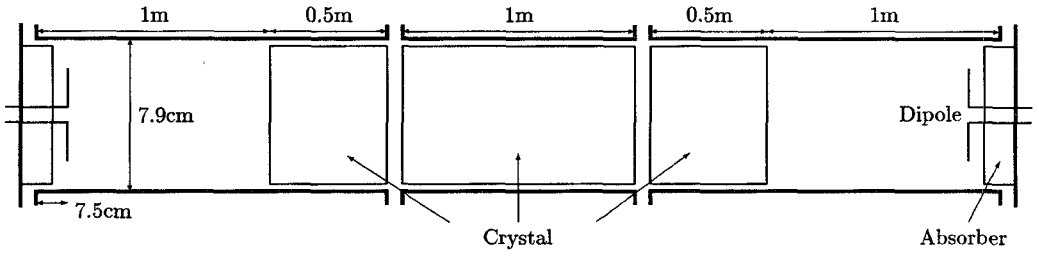

Fig. 3. Schematic representation of the waveguide.

V. The Experiment

The antennas of the experimental system were designed to excite or receive a linearly polarized field along a centerline of the waveguide cross-section and to act as transitions between the coaxial cables connected to the network analyzer and the waveguide containing the sample.

Each antenna was a thin microstrip dipole with length about 70 mm, about 90% of the waveguide diameter, made on a thin dielectric substrate by photolithography. The dipole was connected, without balun, to a semirigid coaxial cable. It was established by free-space pattern measurements and a waveguide cross-polarization measurement that a balun was not necessary. The coaxial feed passed through a 28-mm layer of polystyrene and a 45-mm layer of absorbing material, to minimize multiple reflections, before going through a ground plane that was attached to the end of the waveguide. The resulting structure is round and fits snugly in the pipe, allowing it to center itself as it is turned.

Both antennas are placed in air filled, thus nominally "free-space," regions of the guide, on either side of the chiral crystal. Thus the transmitting antenna will strongly excite the dominant TE_{11} mode. In the empty waveguide the lowest higher mode that can be excited by a balanced antenna is the TM_{11} mode. This corresponds to the T_{12} mode which will not propagate at frequencies below 4.2 GHz in the crystal, and in the free-space section its cut-off frequency will be even higher. Thus, provided the frequency is limited to below 4.2 GHz and the antennas are well balanced, higher order modes will not have a significant effect on the measurements. The resulting theoretical rotation, calculated between 2.2 and 4 GHz, is shown in Fig. 8.

A waveguide was made of a 4 m length of aluminum pipe with inside diameter 79 mm cut into three lengths as shown in Fig. 3 and connected using flanges which allowed the sections of pipe to be flush with each other. When measuring a rotation angle of 10°—which was the expected rotation at 3 GHz—the component orthogonal to the incident polarization will be about 15 dB lower than the component parallel to the incident polarization. Thus it was required that, when exciting a TE_{11} mode in the empty waveguide, the component orthogonal (the cross-polarized component) to the incident polarization plane must be more than 25 dB less than the component in parallel to it. The final assembly had an isolation of 30 to 45 dB with the incident field polarized in the region of four distinct angles labeled $\phi = 0°, 75°, 180°$ and 255°. (The isolation for other angles was worse, due to waveguide imperfections.) The measured data were defined as the average of four individual sets of data where the measurement for each angle was done with the transmit and receive antenna oriented at one of the above angles, and then repeated with the receive antenna rotated through 180°.

The crystal was constructed by embedding the prefabricated chiral structures in a 79.5 mm diameter closed cell Polyfoam disk. The lattice and orientation of the structures are shown in Fig. 4. Each precut disk, 4.13 mm thick, was punctured using a tool made with needles in all the hole positions. The structures, cut and bent beforehand from phosphor-bronze wire, were then hooked through the disks. The foam was flexible enough for the bends to go through without any damage to either the wires or the foam. This was done by hand by a number of students. The disks dented slightly inwards to the thickness corresponding to the length of the z-axis leg, keeping the x- and y-axis legs in approximate registration. Each disk contained a small notch to allow alignment. These disks were alternated with 5.17 mm thick spacers and the whole crystal was glued together with a contact spray in sections of about 200 mm long. A thin plastic tape was wound round the full circumference to ohmically isolate the outer structures from the waveguide wall. It further compressed the slightly oversized disks allowing the crystal to slide into the waveguide without too much friction. Photographs of the construction are shown in Fig. 5.

VI. Results

Fig. 6 shows the copolarized electric field measured by the receive antenna when oriented at an angle, ϕ, relative to the polarization of the incident mode. The measurement was done at 3 GHz with and without the 2 m long crystal in place. The shift caused by the chiral activity can clearly be seen. The pattern follows the sinusoidal distribution expected for a linearly polarized field, with the depth of the nulls indicating that both fields are highly linearly polarized. It can therefore be assumed that there is very little corruption due to higher order modes. This assumption applies through the whole frequency band between 2.4 and 4 GHz.

The amplitude of the wave after propagating through the chiral medium is about 1 dB lower than for the empty waveguide, due to losses in the medium. This attenuation does not significantly affect the experimental results, although the analysis was done for a lossless medium.

In Fig. 7 the magnitude of the field transmitted through the crystal is plotted as a function of frequency for various angles of the receive antenna. These graphs shows clearly the "rotatory dispersion" first viewed by Arago and Biot in 1811

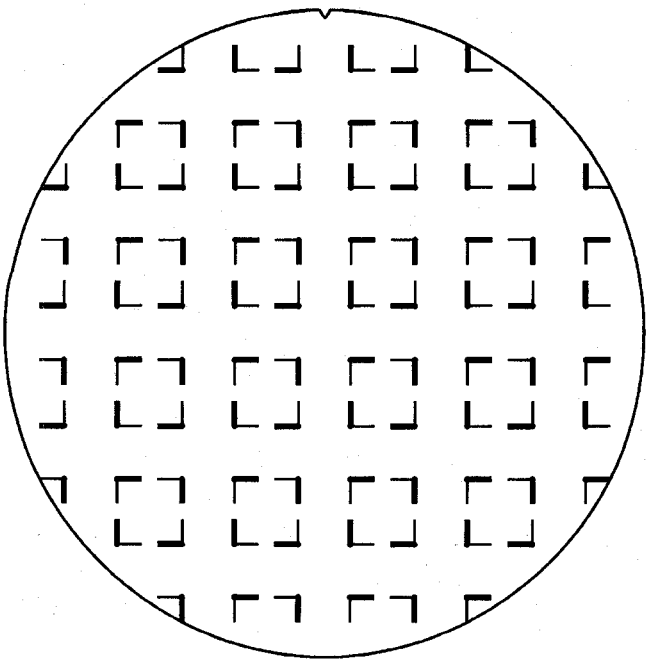

Fig. 4. Disklike building element of the crystal. Only the thick lines are visible from the front of each disk. The thin lines are at the back of the disk.

and 1812 [34] since it is evident that the higher the frequency, the higher the rotation of the null position. The angle ϕ in the figure indicates the amount by which the receive antenna is rotated away from its "null" position in the empty waveguide.

The rotation angle as function of frequency was measured in two different ways. A direct mechanical measurement was obtained by searching for the transmission null and reading the angle from a degree scale on the back of the antenna with 0° corresponding to the null position for the empty guide. The angle was also computed from the amplitude and phase of the measured transmitted E_x and E_y components, by applying the polarization ellipse theory [35, pp. 19–21]. While the mechanical positioning error is estimated to be about 1° to 2° for arbitrary angles, it is possible to align the antennas very precisely in the ±90° orientations by searching for the null in the empty waveguide—thus the "computed" rotation angle is presumably more accurate than the mechanical one. In Fig. 8 both measurements are compared with the theoretical predictions.

The transmission (S_{21}) measurements were made using an HP 8510C network analyzer. Calibration was done with the empty waveguide and a 3.5 ns time domain gate was employed to reduce the effect of multiple reflections in the waveguide and transitions.

VII. Discussion of the Results

Scaling of the theoretical prediction reveals that the discrepancy between the measurement and original prediction is around 13%. This factor is almost constant over the entire frequency band—thus the circular birefringence of the artificial crystal is accurately predicted with an apparent error of approximately 13% in the numeric values of the medium parameters. There is a slight deviation from this frequency behavior below 2.6 GHz and above 3.8 GHz which is probably due to the time domain gating applied to the measurements.

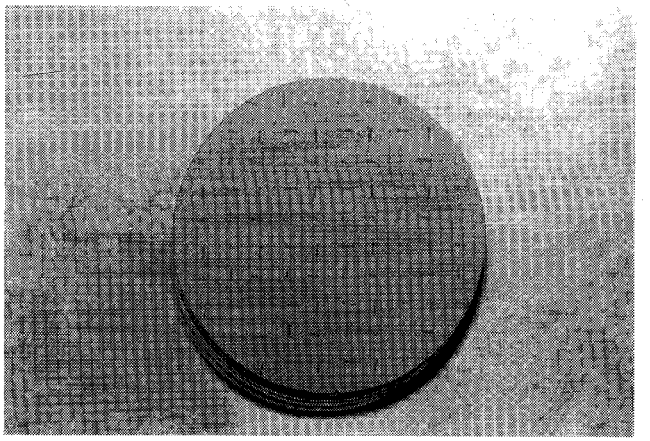

(a)

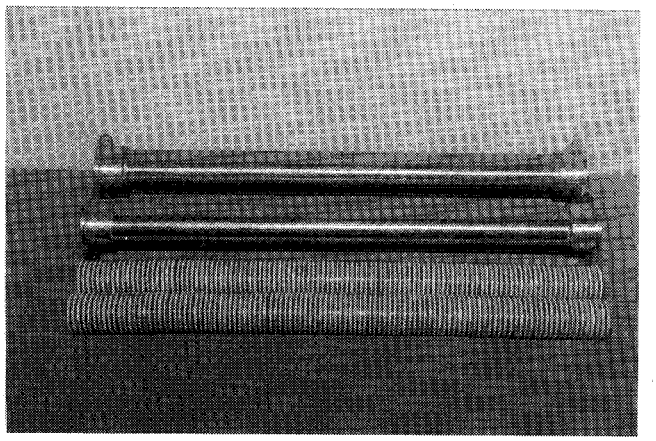

(b)

Fig. 5. Two 1 m long sections of the crystal. The chiral hooks are mounted in the dark disks, and the white disks act as spacers. The other photograph shows the orientation of the chiral hooks on the surface of a disk, and the grooves in the edge of each disk for registration purposes.

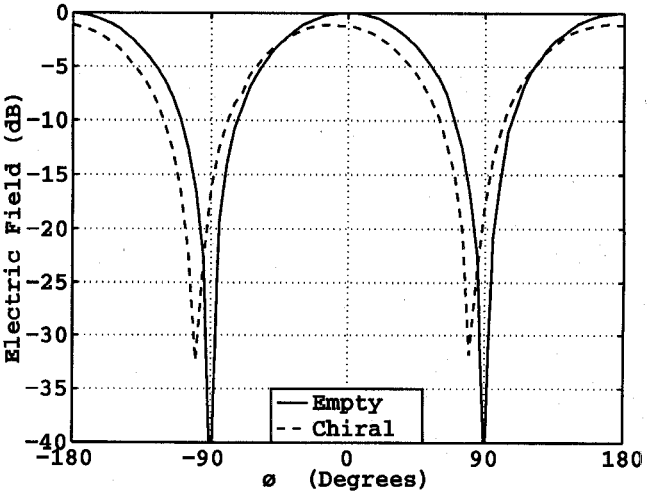

Fig. 6. The solid graph shows the copolarized component of the transmitted electric field measured with the receive antenna oriented at the angle ϕ relative to the incident polarization direction in the empty guide. The dashed graph was obtained at 3 GHz for a wave propagating down the waveguide when filled with the 2 m long crystal.

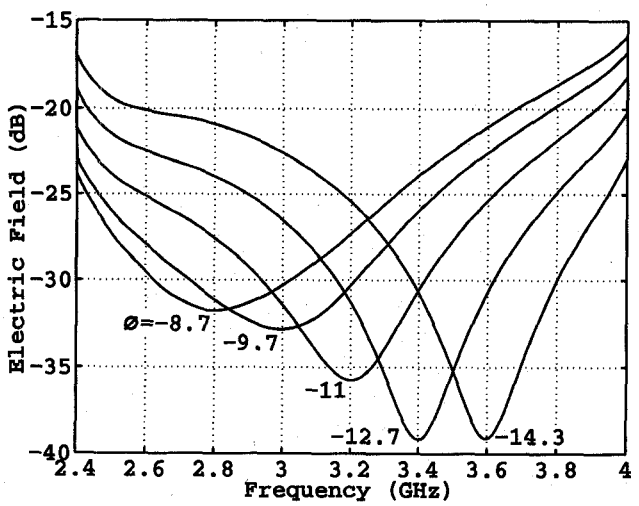

Fig. 7. The amplitude of the copolarized electric field as a function of frequency with the receive antenna at different angles of rotation. The angle ϕ represents the angle by which the receive antenna is rotated away from its null, the cross-polarized position of the empty waveguide. (These angles are found by averaging the different measurements.) The crystal is 2 m long.

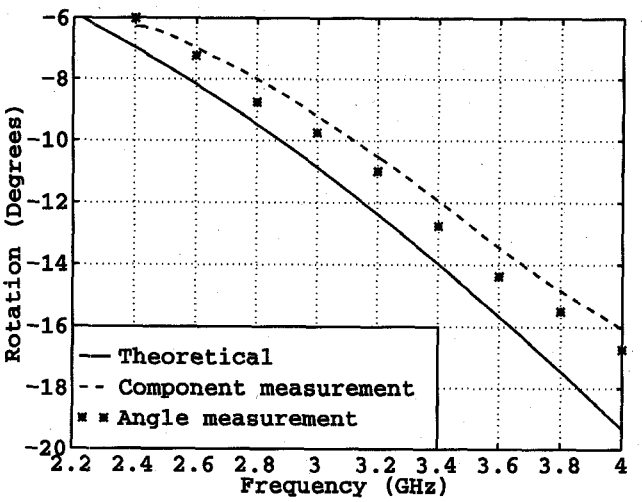

Fig. 8. Comparison of theoretical and measured rotation angle, ϕ_{rot}. The crystal, with the parameters given in the paper, is 2 m long. If the quadrupole is ignored in the theoretical predictions, the predicted rotation would be approximately half of the value given here.

In seeking the cause of the discrepancy there are a number of possible error sources that need to be evaluated [15]. Since the frequency dependence is accurately predicted the fact that the multipole moments were computed using a quasistatic technique [19] probably does not yield a significant contribution to the error. The multipole moments of the single structures were computed using a thin-wire technique which, when compared to a body of revolution code for the test case of a straight dipole, yielded an error of about 3% [15, 19]. A significant error is caused by the fact that the structures which fall partially out of the circle shown in Fig. 4 could not be incorporated in the physical disks—there are in fact 6% less elements than required to yield the volume density used to calculate the parameters. A further error is caused by the alignment of the structures on the crystal lattice. In an isotropic or "random" medium the contribution of the electric quadrupole is averaged out. The slight deviations from the prescribed lattice, for example a slightly rotated structure or one with a z-leg not perfectly perpendicular to the disk surface, can be considered random and will thus tend to decrease the contribution from the quadrupole term. It also decreases the effective length of the legs—which can have a significant effect as shown in the next paragraph.

One of the largest error sources is the uncertainty in the lengths of the structure legs. It was found by numerical experiment that a length change of 0.1 mm on the x- and y-legs can change the result by as much as 10%. As the manufacturing process resulted in the leg on one side being sharp, there is an uncertainty as to what an equivalent length for a flat end would be. The middle of the 0.2 mm long sharp section was used, and this possibly overestimated the length of a leg with a flat end. (The end-cap yields a contribution of almost 20% and in the case of the sharp point it is physically removed from the geometry [19].)

Most of the significant errors were shown to contribute toward the measured rotation being less than predicted. As the effect of the electric quadrupole and the magnetic dipole are approximately equal, ignoring the quadrupole would lead to a theoretical prediction of about half the present one. Therefore the measured data lie much closer to the prediction with the quadrupole included than without it—even without considering the fact that the errors tend to reduce the measured rotation.

VIII. Conclusion

Chiral or optical activity is a second order effect involving the electric quadrupole and magnetic dipole moments [13], yet the scattering from a single structure is completely dominated by the first order electric dipole field. Further, the field of an individual electric dipole may, in general, also have components orthogonal to the electric field which will contribute to the rotation of the forward scattered electric field. Nevertheless, in a perfect isotropic or a uniaxial medium, the electric dipole contributions will cancel exactly. Since the dipole moment is so dominant in the scattering from a single structure the question arises whether, for a practical, and thus imperfect, anisotropic medium such as the 422 point group crystal considered here, small errors in the alignment of the hooks might not yield electric dipole contributions to circular birefringence in the same order as the scattering by the magnetic dipole and electric quadrupole moments. For a single cell consisting of four rotated elements this might certainly be the case. However, for a macroscopically homogeneous medium, consisting of many thousands of cells, the random error due to the electric dipoles of wrongly aligned structures will tend to cancel each other while the effects due to the magnetic dipoles and the electric quadrupoles will always add—and thus dominate.

A very dilute medium, with low optical activity, was considered to simplify the numerical modeling. For a dense medium a more involved calculation of the multipole moments of a single element would be needed to account for the influence of the neighboring elements but the effect of the

electric quadrupoles would still be comparable to that of the magnetic dipoles. This is a fundamental theoretical fact [12].

A fully dynamic numerical model would be required beyond the long wavelength regime. The implication for the multipole description of the medium properties and the validity of its representation as a continuum has however not been studied.

Circular dichroism would occur in composites with significant conductor and dielectric losses. In this work it is assumed that such losses are negligible but the formulation of Raab and Cloete [13] allows for them to be incorporated.

The good agreement between the theoretically predicted and measured rotation angle as function of frequency has provided convincing experimental support for the contention [13] that a physically sound theoretical description of anisotropic chiral media must take the electric quadrupole term into account. This is also consistent with the theoretical fact that electric quadrupole moments need to be included with magnetic dipole moments to guarantee that the medium parameters are independent of the arbitrary origin to which the multipoles are referred [12].

Appendix
Calculating the Fields in a Waveguide

In this Appendix the simultaneous solution of Maxwell's equations is considered

$$\nabla \times \vec{E} = -j\omega\vec{B} \tag{5}$$

$$\nabla \times \vec{H} = j\omega\vec{D} \tag{6}$$

and the constitutive relations

$$\vec{D} = \bar{\epsilon}\cdot\vec{E} + j\bar{\xi}\cdot\vec{B} \tag{7}$$

$$\vec{H} = j\bar{\xi}^T\cdot\vec{E} + \mu_o^{-1}\vec{B} \tag{8}$$

where

$$\bar{\epsilon} = \begin{bmatrix} \epsilon_{xx} & 0 & 0 \\ 0 & \epsilon_{xx} & 0 \\ 0 & 0 & \epsilon_{zz} \end{bmatrix} \quad \bar{\xi} = \begin{bmatrix} \xi_{xx} & \xi_{xy} & 0 \\ -\xi_{xy} & \xi_{xx} & 0 \\ 0 & 0 & \xi_{zz} \end{bmatrix}$$

subject to the boundary condition, $E_z = 0$ at $r = a$, for a general uniaxial medium inside a waveguide. This yields the fields inside the waveguide in terms of an integer parameter, n, that must be chosen and the constant of propagation, β, that is found by solving the boundary condition, $E_\phi = 0$ at $r = a$. The constitutive relations as defined here remain valid for both Cartesian and cylindrical vectors, thus since the boundary conditions are cylindrical, this form is used here.

With an assumed z-dependence of $e^{-j\beta z}$ it is a simple matter to express B_r and B_ϕ in terms of the components of $\vec{E}$ using the r- and ϕ-components of (5). This can be substituted in the constitutive relations and then into the r- and ϕ-components of (6) to find E_r and E_ϕ in terms of E_z and B_z. Then the z-components of the two Maxwell equations yield two equations which can be solved for $\nabla_t^2 E_z$ and $\nabla_t^2 B_z$ to obtain

$$\nabla_t^2 E_z + b_1 E_z + jb_2 B_z = 0 \tag{9}$$

$$\nabla_t^2 B_z + jb_3 E_z + b_4 B_z = 0 \tag{10}$$

where

$$k_\beta^2 = \epsilon_{xx}\mu_o\omega^2 - \beta^2$$

$$b_1 = \frac{\epsilon_{zz}k_\beta^2}{\epsilon_{xx} + \xi_{xy}^2\mu_o}$$

$$b_2 = \frac{k_\beta^2(\xi_{xx} + \xi_{zz}) + 2\beta\xi_{xx}(\beta + j\xi_{xy}\mu_o\omega)}{\epsilon_{xx} + \xi_{xy}^2\mu_o}$$

$$b_3 = -\epsilon_{zz}\mu_o\frac{k_\beta^2(\xi_{xx} + \xi_{zz}) + 2\beta\xi_{xx}(\beta - j\mu_o\omega\xi_{xy})}{\epsilon_{xx} + \xi_{xy}^2\mu_o}$$

$$b_4 = \mu_o\frac{4\beta^2\xi_{xx}\xi_{zz} + k_\beta^2(\xi_{xx} + \xi_{zz})^2}{\epsilon_{xx} + \xi_{xy}^2\mu_o} + k_\beta^2.$$

Similar differential equations for a medium containing sources were obtained by Olyslager *et al.* [36] who then decompose the sources into their TE and TM parts. In the case of anisotropic media the simple Bohren decomposition[1] $\vec{F}_\pm = \vec{E} \pm j\eta\vec{H}$, used for example in [21], no longer applies. Here the separation is done by linearly combining (10) and (9) as follows:

$$\nabla_t^2(E_z - jfB_z) + (b_1 + fb_3)E_z + j(b_2 - fb_4)B_z = 0$$

$$\nabla_t^2(E_z - jgB_z) + (b_1 + gb_3)E_z + j(b_2 - gb_4)B_z = 0.$$

[1] Actually a similar form was introduced in 1907 by Silberstein. See [37, p. 32].

$$k_f = \sqrt{b_1 + f'}$$

$$k_g = \sqrt{b_1 + g'}$$

$$f' = b_3 f = \frac{k_\beta^2(\epsilon_{xx} - \epsilon_{zz}) + 4\mu_o\beta^2\xi_{xx}\xi_{zz} + \mu_o k_\beta^2(\xi_{xx} + \xi_{zz})^2 + b_5}{2\epsilon_{xx}}$$

$$g' = b_3 g = \frac{k_\beta^2(\epsilon_{xx} - \epsilon_{zz}) + 4\mu_o\beta^2\xi_{xx}\xi_{zz} + \mu_o k_\beta^2(\xi_{xx} + \xi_{zz})^2 - b_5}{2\epsilon_{xx}}$$

$$b_1 = \frac{\epsilon_{zz}k_\beta^2}{\epsilon_{xx}}$$

$$b_2 = \frac{2\beta^2\xi_{xx} + k_\beta^2(\xi_{xx} + \xi_{zz})}{\epsilon_{xx}}$$

$$b_5 = \sqrt{(k_\beta^2(\epsilon_{xx} + \epsilon_{zz}) + 4\mu_o\beta^2\xi_{xx}\xi_{zz} + \mu_o k_\beta^2(\xi_{xx} + \xi_{zz})^2)^2 - 4\epsilon_{xx}\epsilon_{zz}(k_\beta^4 - 4\mu_o^2\omega^2\beta^2\xi_{xx}^2)}$$

The new equations will be independent of each other provided that $f \neq g$. Substituting $F = E_z - jfB_z$ and $G = E_z - jgB_z$ yields separated equations on condition that

$$b_2 - (b_4 - b_1)f + b_3 f^2 = b_2 - (b_4 - b_1)g + b_3 g^2 = 0$$

which gives the same two possible solutions for f and g. The requirement $f \neq g$ can be met by selecting one solution for f and the other for g

$$f = \frac{b_4 - b_1 + \sqrt{(b_4 - b_1)^2 - 4b_2 b_3}}{2b_3}$$
$$g = \frac{b_4 - b_1 - \sqrt{(b_4 - b_1)^2 - 4b_2 b_3}}{2b_3}$$

such that

$$\nabla_t^2 F + (b_1 + f b_3)F = \nabla_t^2 F + k_f^2 F = 0 \tag{11}$$
$$\nabla_t^2 G + (b_1 + g b_3)G = \nabla_t^2 G + k_g^2 G = 0. \tag{12}$$

The general solution of this equation in cylindrical coordinates is

$$A_1 J_\nu[kr]e^{j\nu\phi} + A_2 \mathrm{Y}_\nu[kr]e^{j\nu\phi}$$

where $k = k_f$ for the solution of (11) and $k = k_g$ for that of (12). J_v and Y_v are the Bessel functions of the first and second kind of order v. Since the solution must be continuous in ϕ and remain bounded at $r \to 0$, it can be simplified to

$$F = A_1 J_n[k_f r]e^{jn\phi}$$
$$G = A_2 J_n[k_g r]e^{jn\phi}$$

where $n = 0, \pm 1, \pm 2, \pm 3, \cdots$

Setting $E_z = 0$ at $r = a$ and realising that E_z is proportional to $fG - gF$ yields

$$A_2 = \frac{g J_n[k_f a]}{f J_n[k_g a]} A_1$$

from which F and G can be found. This yields the fields which, after scaling and using Bessel identities to avoid singularities, can be written as

$$E_r = jA\{J_n[k_g a](h_1 J_{n-1}[k_f r] + h_2 J_{n+1}[k_f r]) - J_n[k_f a](h_3 J_{n-1}[k_g r] + h_4 J_{n+1}[k_g r])\}e^{j(n\phi - \beta z)} \tag{13}$$

$$E_\phi = -A\{J_n[k_g a](h_1 J_{n-1}[k_f r] - h_2 J_{n+1}[k_f r]) - J_n[k_f a](h_3 J_{n-1}[k_g r] - h_4 J_{n+1}[k_g r])\}e^{j(n\phi - \beta z)} \tag{14}$$

$$E_z = 2h_0 A\{J_n[k_f a]J_n[k_g r] - J_n[k_g a]J_n[k_f r]\}e^{j(n\phi - \beta z)} \tag{15}$$

where

$$h_0 = b_2(k_\beta^4 - 4\mu_o^2\omega^2\beta^2\xi_{xx}^2)$$
$$h_1 = k_f(k_\beta^2 - 2\mu_o\omega\beta\xi_{xx})(\omega b_3 f + b_2\beta - \mu_o\omega b_2(\xi_{xx} + \xi_{zz} + j\xi_{xy}))$$
$$h_2 = k_f(k_\beta^2 + 2\mu_o\omega\beta\xi_{xx})(\omega b_3 f - b_2\beta - \mu_o\omega b_2(\xi_{xx} + \xi_{zz} - j\xi_{xy}))$$
$$h_3 = k_g(k_\beta^2 - 2\mu_o\omega\beta\xi_{xx})(\omega b_3 g + b_2\beta - \mu_o\omega b_2(\xi_{xx} + \xi_{zz} + j\xi_{xy}))$$
$$h_4 = k_g(k_\beta^2 + 2\mu_o\omega\beta\xi_{xx})(\omega b_3 g - b_2\beta - \mu_o\omega b_2(\xi_{xx} + \xi_{zz} - j\xi_{xy}))$$

for the general uniaxial medium. For the medium discussed in this paper, $\xi_{xy} = 0$, such that the constants b_2, k_f, etc. are given by the simplified equations shown at the bottom of the previous page.

REFERENCES

[1] D. L. Jaggard, A. R. Mickelson, and C. H. Papas, "On electromagnetic waves in chiral media," *Appl. Physics*, vol. 18, pp. 211–216, 1979.

[2] A. Lakhtakia, V. K. Varadan, and V. V. Varadan, *Time-Harmonic Electromagnetic Fields in Chiral Media, Lecture Notes in Physics 335*. Berlin: Springer-Verlag, 1989.

[3] I. V. Lindell, A. H. Sihvola, S. A. Tretyakov, and A. J. Viitanen, *Electromagnetic Waves in Chiral and Bi-Isotropic Media*. Boston: Artech House, 1994.

[4] E. J. Post, *Formal Structure of Electromagnetics*. Amsterdam, The Netherlands: North-Holland, 1962.

[5] H. Nakano and H. Kimura, "Quantum statistical-mechanical theory of optical activity," *J Phys. Soc. Japan*, vol. 27, no. 3, pp. 519–535, 1969. Reprinted in [38], pp. 362–378.

[6] A. D. Buckingham and M. B. Dunn, "Optical activity of oriented molecules," *J Chemical Soc. A*, pp. 1988–1991, 1971.

[7] P. S. Reese and A. Lakhtakia, "A periodic chiral arrangement of thin identical bianisotropic sheets: Effective properties," *Optik*, vol. 86, no. 2, pp. 47–50, 1990.

[8] R. D. Graglia, P. L. E. Uslenghi, and R. E. Zich, "Dispersion relation for bianisotropic materials and its symmetry properties," *IEEE Trans. Antennas Propagat.*, vol. 39, no. 1, pp. 83–90, 1991.

[9] I. V. Lindell and A. J. Viitanen, "Plane wave propagation in a uniaxial bianisotropic medium," *Electronics Lett.*, vol. 29, no. 2, pp. 150–152, 1993.

[10] I. V. Lindell and W. S. Weiglhofer, "Green dyadic and dipole fields for a medium with anisotropic chirality," *IEE Proc-H*, vol. 141, no. 3, pp. 211–215, 1994.

[11] A. Lakhtakia, "Scaling of fields, sources and constitutive properties in bianisotropic media," *Microwave Opt. Technol. Lett.*, vol. 7, no. 7, pp. 328–330, 1994.

[12] E. B. Graham, J. Pierrus, and R. E. Raab, "Multipole moments and Maxwell's equations," *J Physics B*, vol. 25, pp. 4673–4684, 1992.

[13] R. E. Raab and J. H. Cloete, "An eigenvalue theory of circular birefringence and dichroism in a nonmagnetic chiral medium," *J Electromagnetic Waves Applicat.*, vol. 8, no. 8, pp. 1073–1089, 1994.

[14] E. B. Graham and R. E. Raab, "Reflection from noncentrosymmetric uniaxial crystals: a multipole approach," *J. Opt. Soc. Am. A*, accepted Oct. 1995. (Further details are available in: E. B. Graham and R. E. Raab, "New insights into the Maxwell boundary condition: Application to a chiral medium," private communication. Submitted for publication, 1 Mar. 1995.)

[15] I. P. Theron, *The Circular Birefringence of Artificial Chiral Crystals at Microwave Frequencies*, Ph.D. dissertation, Dep. Elec. and Electron. Eng., Univ. of Stellenbosch, Oct. 1995.

[16] I. P. Theron and J. H. Cloete, "The optical activity of an artificial nonmagnetic uniaxial chiral crystal at microwave frequencies," *J Electromagnetic Waves Applications*, vol. 10, no. 4, pp. 539–561, 1996.

[17] W. C. Chew, *Waves and Fields in Inhomogeneous Media*. New York: Van Nostrand, 1990.

[18] R. R. Birss, *Symmetry and Magnetism*, 2nd ed. Amsterdam, The Netherlands: North-Holland, 1966.

[19] I. P. Theron, D. B. Davidson, and J. H. Cloete, "Computation of multipole moments for short thin wire chiral structures," *Appl, Computational Electromagnetics Soc, J,*, vol. 10, no. 3, pp. 129–138, 1995.
[20] P. Pelet and N. Engheta, "The theory of chirowaveguides," *IEEE Trans. Antennas Propagat,*, vol. 38, no. 1, pp. 90–98, 1990.
[21] C. Eftimiu and L. W. Pearson, "Guided electromagnetic waves in chiral media," *Radio Sci,*, vol. 24, no. 3, pp. 351–359, 1989.
[22] T. C. K. Rao, "Attenuation characteristics of a circular chirowaveguide," *Electronics Lett,*, vol. 26, no. 21, pp. 1767–1769, 1990.
[23] R. D. Hollinger, V. V. Varadan, and V. K. Varadan, "Eigenmodes in a circular waveguide containing an isotropic chiral material," *Radio Sci,*, vol. 26, no. 5, pp. 1335–1344, 1991.
[24] H.-Y. Yang and P. L. E. Uslenghi, "Planar bianisotropic waveguides," *Radio Sci,*, vol. 28, no. 5, pp. 919–927, 1993.
[25] M. M. I. Saadoun and N. Engheta, "A reciprocal phase shifter using novel pseudochiral or Omega medium," *Microwave and Optical Technology Letters*, vol. 5, no. 4, pp. 184–188, 1992.
[26] Y. Xu and R. G. Bosisio, "An efficient method for study of general bi-anisotropic waveguides," *IEEE Trans. Microwave Theory and Techniques*, vol. 43, no. 4, pp. 873–879, 1995.
[27] J. A. M. Svedin, "Propagation analysis of chirowaveguides using finite-element method," *IEEE Trans. Microwave Theory Tech.*, vol. 38, no. 10, pp. 1488–1496, 1990.
[28] A. R. Samant and K. W. Whites, "Electromagnetic wave propagation in a chiral–material–filled rectangular waveguide," *Microwave Opt. Technol. Lett.*, vol. 8, no. 2, pp. 106–111, 1995.
[29] H. Cory, "Wave propagation along a closed rectangular chirowaveguide," *Microwave Opt. Technol. Lett.*, vol. 6, no. 14, pp. 797–800, 1993.
[30] P. J. B. Clarricoats and B. C. Taylor, "Evanescent and propagating modes of dielectric-loaded circular waveguide," *Proc. IEE*, vol. 111, no. 12, pp. 1951–1956, 1964.
[31] A. R. Samant and K. W. Whites, "Notable features of hybrid modes in a chiral–filled rectangular waveguide," *IEEE Microwave Guided Wave Lett.*, vol. 5, no. 5, pp. 144–146, 1995.
[32] G. Busse and A. F. Jacob, "Complex power and mode coupling in circular chirowaveguides," *IEEE Trans. Microwave Theory Tech.*, vol. 43, no. 5, pp. 1182–1186, 1995.
[33] K. W. Whites and R. Mittra, "Complex and backward-wave modes in dielectrically loaded lossy circular waveguides," *Microwave Opt. Technol. Lett.*, vol. 2, no. 6, pp. 199–204, 1989.
[34] J. Applequist, "Optical activity: Biot's bequest," *American Scientist*, vol. 75, no. 1, pp. 58–68, 1987.
[35] J. A. Kong, *Electromagnetic Wave Theory*. New York: Wiley, 1986.
[36] F. Olyslager, B. Jakoby, and I. V. Lindell, "TE-TM source decomposition for general uniaxial bianisotropic media," *Microwave Optical Technol. Lett.*, vol. 9, no. 6, pp. 345–349, 1995.
[37] J. A. Stratton, *Electromagnetic Theory*. New York: McGraw-Hill, 1941.
[38] A. Lakhtakia, Ed., *Selected Papers on Natural Optical Activity*. Bellingham, WA: SPIE—The International Society for Optical Engineering, 1990.

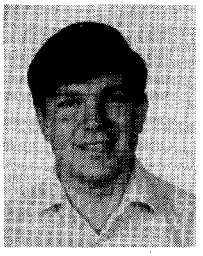

Isak Petrus Theron was born in 1967 and grew up in Upington, South Africa. He received the B.Eng. and M.Eng. degrees, both *cum laude*, and the Ph.D. (Eng.) degree from the University of Stellenbosch in 1989, 1991, and 1995, respectively.

He is presently a Post-Doctoral Fellow in the electromagnetics group of the Department of Electrical and Electronic Engineering at Stellenbosch. His doctoral research was directed at modeling anisotropic chiral media by combining optical theories of matter from molecular physics with the analytical, numerical and experimental techniques of classical electromagnetics. He is currently working on industrial applications of antenna analysis, design and measurements.

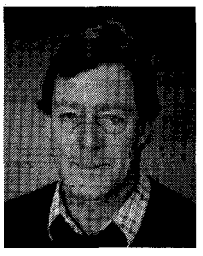

Johannes Hendrik Cloete was born in Clocolan, Orange Free State, South Africa in 1945. He received the B.Sc., B.Eng. and Ph.D. (Eng) degrees in electrical engineering from the University of Stellenbosch and the M.S. degree in electrical engineering from the University of California, Berkeley.

He has been a Professor in the Department of Electrical and Electronic Engineering at the University of Stellenbosch since 1984. His research interests are the electromagnetic properties of materials, experimental and analytical methods for characterizing them, and antenna engineering.